

Late time accelerated scaling attractors in DGP (Dvali-Gabadadze-Porrati) braneworld

Jibitesh Dutta^{1*}, Wompherdeiki Khylllep^{2†}, Erickson Syiemlieh^{2‡}

¹*Mathematics Division, Department of Basic Sciences and Social Sciences,
North Eastern Hill University, NEHU Campus,
Shillong - 793022, Meghalaya (INDIA) and*

²*Department of Mathematics, St. Anthony's College, Shillong - 793001, Meghalaya (INDIA)*

(Dated: June 11, 2022)

In the evolution of late universe, the main source of matter are Dark energy and Dark matter. They are indirectly detected only through their gravitational manifestations. So the possibility of interaction with each other without violating observational restrictions is not ruled out. With this motivation, we investigate the dynamics of DGP braneworld where source of dark energy is a scalar field and it interacts with matter source. Since observation favours phantom case more, we have also studied the dynamics of interacting phantom scalar field. In non interacting DGP braneworld there are no late time accelerated scaling attractors and hence cannot alleviate Coincidence problem. In this paper, we shall show that it is possible to get late time accelerated scaling solutions. The phase space is studied by taking two categories of potentials (Exponential and Non exponential functions). The stability of critical points are examined by taking two specific interactions. The first interaction gives late time accelerated scaling solution for phantom field only under exponential potential, while for second interaction we do not get any scaling solution. Furthermore, we have shown that this scaling solution is also classically stable.

I. INTRODUCTION

The fact that our universe is currently undergoing an accelerated expansion has been confirmed by many observations since last fifteen years [1–4]. In standard cosmology, this accelerated expansion can be explained by dark energy(DE). It is an exotic entity with negative pressure. One of the most simple contender for DE is the time-independent cosmological constant (Λ) whose equation of state (EOS) ω is equal to -1 . But this suffer from well known Coincidence Problem - why DE and Dark matter (DM) energy densities are of same order at present even though they evolve at a highly different red-shift [5, 6]. The cosmological constant problem can also be alleviated by modelling DE with a scalar field whose equation of state varies dynamically. Scalar fields play a crucial role in cosmology because they are simple and able to generate meaningful dynamics. Canonical scalar fields can be used to model dark energy and inflation[7, 8]. Dynamical scalar field models such as Quintessence ($-1 < \omega < -\frac{1}{3}$)[9], K-essence [10], Phantom fields ($\omega < -1$) [11] etc were proposed as possible candidates for DE. For a review on different cosmological dark energy models see [12, 13]. These models have some merits over the cosmological constant problem. Furthermore, these models yield observed values of ω and can mimic cosmological constant at present epoch.

Generally, in cosmological models where scalar fields are used to describe DE, the background matter does not interact with scalar field. But there is no principle of physics by which this interaction of DE and DM can be ruled out. We may get similar energy density in the dark sector if there is an interaction of DE and DM. So the main motivation for taking interaction between DE and DM is to alleviate the coincidence problem. Since the nature of DE and DM is still unknown, so currently there is no specific form interaction. Therefore, any interaction considered is phenomenological one, even though some may have better justification over the others.

The first interaction between scalar field and matter and its various ramifications are studied in [14, 15]. The main advantage of interaction of quintessence and DM is that scaling solutions can lead to late time acceleration [15, 16]. This cannot be obtained without considering interaction. Furthermore, attempts have been made to study the dynamics of interacting phantom fields and DM[17, 18].

The recent accelerated expansion of the universe can also be explained by theories of extra dimensions. Braneworld scenario is an important theory of extra dimension inspired by string theory. In this set up, our observable universe is a hyperspace (called brane) embedded in a higher dimensional space-time known as bulk. Braneworld models correct standard cosmology in a noble way and solve many outstanding problems of cosmology. Moreover, it has some important differences from standard cosmology and one can see the standard review in [19].

DGP braneworld (proposed by Dvali, Gabadadze and Porrati) is one of the promising theory of braneworld [20, 21]. It consists of two branches, one of which is the self-accelerating branch which does not need any DE for

* jdutta29@gmail.com, jibitesh@nehu.ac.in

† sjwomkhylllep@gmail.com

‡ eric.syiem@gmail.com

acceleration and the other is the normal branch which requires DE to accelerate. But the former suffers from the ghost problem while the latter is free from ghost instabilities. Usually phantom fluid is known to violate Weak Energy Condition (WEC) but in DGP (normal branch) model the phantom characteristic of violating WEC is suppressed by brane gravity effects. Another interesting feature of this brane world model is violation of Strong Energy Condition (SEC) and as a result this model accelerates [22].

Moreover, in the normal branch of DGP model, the generalized second law of thermodynamics (GSLT) is satisfied at both apparent and event horizon (with some reasonable restrictions) and as a result this model is a perfect thermodynamical system [23]. It may be noted GSLT is an inherent property of any cosmological model and it should be valid throughout the evolution. In order to have validity of GSLT at event horizon for self accelerating branch some interaction between dark matter and dark DE has to be considered [24]. So interaction between dark sectors can also alleviate problems from thermodynamical point of view.

Furthermore, in literature different modified DGP models have been studied. One of the simplest is the LDGP model where the source of DE is taken to be cosmological constant [25, 26]. Some of the other modified DGP models include the following: (i) QDGP model where source of DE is a quintessence field [27]. (ii) CDGP model where source of DE is a Chaplygin Gas [28]. (iii) SDGP model where source of DE is a scalar field [29]. (iv) HDGP model where source of DE is a holographic dark energy [30] etc.

Dynamical system study has been found to be very useful in cosmology [31, 32]. The objective of dynamical system tool is to study the asymptotic behaviour of cosmological models. Stable point of the system corresponds to ultimate fate of universe. Such points are also called as late-time attractors. In other words, late time attractors give possible solution which describe our present universe irrespective of initial conditions. Recently, the interacting DE models from dynamical systems perspective have been extensively studied in literature [33–38].

Scaling solutions play an important role in constructing models of DE [39–41] and are desirable in cosmic evolution. Here density of the scalar fields dominate at late time only and remains sub dominant at early time. In general, GR (General Relativity) based scalar field models of DE do not admit scaling attractor unless interaction is considered between dark sectors [33]. In standard cosmology scaling solution are generally unstable for phantom fields. Guo *et al* have shown that it is possible to get stable scaling solutions through interacting phantom energy model [34].

Dynamical evolution of self accelerating scalar field with constant and exponential potential trapped on the DGP brane has been studied in [42]. This study has been extended to beyond constant and exponential potentials by Leyva *et al* [43]. Cosmological dynamics of quintessence and phantom field with exponential potential coupled to gravity (minimal and non-minimal) in DGP brane has been studied in [44]. It is noted that in all these studies, there is no late time accelerated scaling attractors. The aim of this paper is to search for late time accelerated scaling attractors in DGP braneworld.

In this paper, we investigate the dynamics of scalar field (quintessence/phantom) which interacts with matter source in DGP braneworld. In GR based models, the late time accelerated scaling attractors are present only in interacting quintessence models. We shall show that it is possible to get late time accelerated scaling attractors for phantom case in DGP braneworld. Moreover, we have also investigated the classical stability of the model and found that these attractors are also classically stable.

The organization of the paper is as follows: In sect. II we present the basic equations of interacting DGP braneworld model and the formation of autonomous system of differential equations. In sect. III we discuss the local and classical stability of critical points obtained and finally, the conclusion is given in sect. IV.

II. BASIC EQUATION OF DGP BRANEWORLD AND FORMATION OF DYNAMICAL SYSTEM

The total action of the scalar field in DGP braneworld model with matter is given by

$$S = \frac{M_5^3}{2} \int d^5x \sqrt{-g^{(5)}} R^{(5)} + \int \left[\frac{M_{Pl}^2}{2} R - \theta \frac{1}{2} g^{\mu\nu} \nabla_\mu \phi \nabla_\nu \phi - V(\phi) + \mathcal{L}_m \right] \sqrt{-g} d^4x \quad (1)$$

where M_5 and M_{Pl} are five dimensional and four dimensional Planck mass respectively, while $g_{\mu\nu}^{(5)}$ and $R^{(5)}$ denote metric and Ricci scalar in the bulk respectively, the corresponding quantity in the brane are denoted by $g_{\mu\nu}$ and R respectively. Here the potential of the scalar field ϕ is denoted by $V(\phi)$ and \mathcal{L}_m is a matter Lagrangian on the brane. Further we note that for $\theta = 1$, we get an ordinary (quintessence) scalar field and $\theta = -1$ corresponds to a phantom field.

Observations support spatially flat [45] Friedmann Robertson Walker (FRW) spacetime, given by the line element

$$ds^2 = -dt^2 + a^2(t)(dx^2 + dy^2 + dz^2) \quad (2)$$

where $a(t)$ is a scale factor.

If we vary (1) with respect to metric tensor components, then we get modified Friedmann equation of DGP model in the above spacetime [20, 21] as

$$H^2 - \epsilon \frac{H}{r_c} = \frac{\rho}{3} \quad (3)$$

where $\epsilon = \pm 1$, $H = \frac{\dot{a}}{a}$ is the Hubble parameter and $r_c = \frac{M_{Pl}^2}{2M_5^3}$ is known as the cross-over scale which differentiates the brane dynamics of universe from the usual 4D universe.

The usual 4D Friedmann equation is obtained when $H^{-1} \ll r_c$, but $H^{-1} \gg r_c$ implies the 5-dimensional effect of gravity. Further $\epsilon = 1$ corresponds to DGP(+) model which is self-accelerating, while for $\epsilon = -1$ we have DGP(-) model which requires DE on the brane to accelerate. In this paper, we study DGP(-) model where the scalar field (quintessence/phantom) is taken as source of DE.

Eq. (3) can also be written as

$$H^2 + \frac{H}{r_c} = \frac{\rho_m + \rho_\phi}{3} \quad (4)$$

where total energy is taken as $\rho_\phi + \rho_m$. Here ρ_ϕ is energy density of scalar field and ρ_m is the energy density of the matter (Baryonic+DM). The matter is taken as a perfect fluid with barotropic equation of state $p_m = (\gamma - 1)\rho_m$ where a constant γ is known as barotropic index of perfect fluid ($0 \leq \gamma \leq 2$). Since DM is the dominant source of matter, therefore for brevity we denote matter source by DM.

Eq. (4) can be written as

$$H^2 = \frac{1}{3}(\rho_m + \rho_{\text{eff}}) \quad (5)$$

where

$$\rho_{\text{eff}} = \rho_\phi - \frac{3H}{r_c} \quad (6)$$

The energy density and pressure of a scalar field are respectively given by

$$\rho_\phi = \theta \frac{1}{2} \dot{\phi}^2 + V(\phi) \quad (7)$$

$$p_\phi = \theta \frac{1}{2} \dot{\phi}^2 - V(\phi) \quad (8)$$

The energy conservation equations for ρ_m , ρ_ϕ are respectively given by

$$\dot{\rho}_m + 3H\gamma\rho_m = -Q \quad (9)$$

$$\dot{\rho}_\phi + 3H(\rho_\phi + p_\phi) = Q \quad (10)$$

where Q is the strength of interaction between DE and DM. The sign of Q determines the direction of energy transfer. For $Q > 0$, energy is transferred from DM to DE and for $Q < 0$ energy is transferred from DE to DM. For $Q = 0$, $\theta = 1$, the study reduce to the case of non-interaction which had been studied in literature [42–44].

Furthermore, we have conservation equation for effective energy density given by

$$\dot{\rho}_{\text{eff}} + 3H(1 + \omega_{\text{eff}})\rho_{\text{eff}} = Q \quad (11)$$

where $\omega_{\text{eff}} = \frac{p_{\text{eff}}}{\rho_{\text{eff}}}$.

From the eqs. (4), (9) and (10) we obtain

$$\frac{\dot{H}}{H^2} = -\frac{3}{2} \left[\frac{(1 + \omega_\phi)\Omega_\phi + \gamma\Omega_m}{1 + \sqrt{\Omega_{r_c}}} \right] \quad (12)$$

From eqs. (6), (10), (11) and (12) we obtain

$$1 + \omega_{\text{eff}} = \frac{\sqrt{\Omega_{r_c}} [(1 + \omega_\phi)\Omega_\phi - \gamma\Omega_m]}{\Omega_{\text{eff}}} \quad (13)$$

where

$$\Omega_{\text{eff}} = \frac{\rho_{\text{eff}}}{3H^2} \quad (14)$$

From eq. (4),

$$1 = \Omega_m + \Omega_\phi - 2\sqrt{\Omega_{r_c}} \quad (15)$$

where $\Omega_m = \frac{\rho_m}{3H^2}$ is dimensionless matter energy density parameter, $\Omega_\phi = \frac{\rho_\phi}{3H^2}$ is dimensionless dark energy density parameter and $\Omega_{r_c} = \frac{1}{4r_c^2 H^2}$ is dimensionless parameter which determines the DGP character.

Using eqs. (7) and (8) in eq.(10), the equation of motion of scalar field is obtained as

$$\ddot{\phi} + 3H\dot{\phi} + \theta \frac{dV}{d\phi} = \frac{\theta Q}{\dot{\phi}} \quad (16)$$

We now introduce the following dimensionless variables

$$x = \frac{\dot{\phi}}{\sqrt{6}H}, \quad y = \frac{\sqrt{V}}{\sqrt{3}H}, \quad z = \frac{1}{\sqrt{2}r_c H}, \quad s = -\frac{1}{V} \frac{dV}{d\phi} \quad (17)$$

Eq. (17) implies that at $z = 0$ corresponds to $r_c \rightarrow \infty$, in which brane effect will vanish and it reduces to standard 4 dimensional behaviour.

The relevant cosmological parameters in terms of dimensionless variables (17) *viz.*, DM energy density parameter, DE density parameter, equation of state parameter for scalar field and deceleration parameter are respectively given by

$$\Omega_m = 1 - \theta x^2 - y^2 + 2z^2 \quad (18)$$

$$\Omega_\phi = \theta x^2 + y^2 \quad (19)$$

$$\omega_\phi = \frac{\theta x^2 - y^2}{\theta x^2 + y^2} \quad (20)$$

$$q = -1 + \frac{3}{2(z^2 + 1)} (2x^2 + \gamma(1 - \theta x^2 - y^2 + 2z^2)) \quad (21)$$

Since $0 \leq \Omega_m \leq 1$, so from eq. (18), we have $\theta x^2 + y^2 \leq 2z^2 + 1$. It may be noted that eqns.(18-21) coincide with those of ref [44] for $\theta = 1$ and $Q = 0$.

We now estimate the initial conditions for numerical solutions in such a way that it matches with present observational data ($\Omega_{r_c} = 0.12, \Omega_m = 0.27$)[46] and present observed value of deceleration parameter $q_0 = -0.61$ [47]. Using eqns. (18) and (21), yield the following lower bound set for the present work.

$$x_0 = \pm 0.20, \quad y_0 = \pm 1.17, \quad z_0 = \pm 0.59 \quad (22)$$

Here, x_0, y_0 and z_0 are present values of x, y and z respectively (*i.e.*, $N = \ln a = 0$).

III. PHASE SPACE ANALYSIS

This section deals with local and classical stability analysis of critical points of a corresponding autonomous system and their cosmological implications. Before going to the discussion of stability of critical points, we review briefly some methods that will be used in this paper.

Let $\mathbf{x}' = \mathbf{f}(\mathbf{x})$ denotes a non-linear autonomous system and \mathbf{x}_* be a critical point *i.e.*, $\mathbf{f}(\mathbf{x}_*) = 0$ where $\mathbf{f} : \mathbb{R}^n \rightarrow \mathbb{R}^n$. The linearised form of a given non-linear system near a critical point can be written as $\mathbf{x}' = A\mathbf{x}$ where $A = \mathbf{Df}(\mathbf{x}_*)$ is the Jacobian matrix of \mathbf{f} at \mathbf{x}_* and $\mathbf{Df}(\mathbf{x}_*) = \left(\frac{\partial f_i}{\partial x_j} \right)$, $i, j = 1, 2, 3, \dots, n$. A critical point is called a *hyperbolic point* if all the eigenvalues of its corresponding Jacobian matrix contains a *non-zero* real components. In this case one can apply linear stability analysis to check the stability of a point [48]. Otherwise it

is a *non-hyperbolic point* where linear stability theory cannot give any valid stability decisions. The perturbation plot is very popular now a days to determine the stability of non hyperbolic critical points [49]. Other known mathematical tools like Centre Manifold Theory, Lyapunov functions [48, 50] can also be used to determine the stability of such critical point. For a set of non-isolated critical points, if its Jacobian matrix contains only one eigenvalue with zero real part and the rest are all non-zero and the eigenvector associated with a zero eigenvalue is tangent to the set of critical points then the set is said to be *normally hyperbolic set* [51]. The stability of this set is determined by the signs of the remaining non-zero eigenvalues. In this present work for non-hyperbolic points we use numerical methods of perturbed solutions around a critical point and normally hyperbolic set property. These methods have been extensively used recently in studying cosmological scenarios[52, 53]. In what follows we choose following two types of specific interactions

$$(A) \quad Q = \sqrt{\frac{2}{3}} \alpha \rho_m \dot{\phi} \quad (B) \quad Q = \beta \dot{\rho}_\phi$$

While interaction A was introduced in [15, 16] and a dynamical study in the context of GR both quintessence and phantom was studied in [33, 54], interaction B was studied recently for quintessence in GR context [38] where coincidence problem is alleviated in comparison to the uncoupled model [39]. These interactions belong to the class of local interactions where both depend directly on the energy density unlike the class of non-local/global interactions which depends on the Hubble parameter and energy density [33].

In order to determine the stability of critical points of an autonomous system, we need to specify form of potentials. The consideration of a specific potential is generally done by ad hoc mechanism. In literature various candidates have been proposed such as inverse power law, exponential, hyperbolic and many more (for review see [12, 55]). Depending on the choice of $\Gamma \equiv \frac{V \frac{d^2 V}{d\phi^2}}{(\frac{dV}{d\phi})^2}$, the potential can be broadly categorised as[56]:

Category I: Non-exponential form, $\Gamma \neq 1$.

In order to study the nature of non-hyperbolic points, we consider one concrete potential $V(\phi) = \frac{M^{4+n}}{\phi^n}$, where M and n are constants for which $\Gamma = 1 + \frac{1}{n}$. This potential can lead to tracking behaviour [57]. Tracker field is very important from coincidence problem point of view as scalar field tracks the background matter energy density throughout the history of the universe and eventually overtakes the matter density to produce late time acceleration.

Category II: Exponential form, $\Gamma = 1$

Exponential potential of scalar field models arise naturally from fundamental theories such as String theory/M-Theory[58]. Exponential potential produce scaling solutions which are desirable from coincidence problem point of view. Exponential potential plays a crucial cosmological role for driving cosmological inflation period [59–61]. In case of exponential potential, we consider $V = V_0 \exp(-\lambda \phi)$. Here we assume $\lambda > 0$ as $\lambda < 0$ can be associated with the change of $\phi \rightarrow -\phi$. The advantage of this potential is that the phase space reduce to three dimension, from which behaviour of a system can be easily studied.

Local stability of a point is related to small perturbations on values of x, y, z and s near a point. Classical stability of a model is related to the fluctuation in dark energy pressure δp_ϕ . In cosmological perturbation theory, the important quantity which plays a key factor for stability of classical fluctuation is the adiabatic speed of sound C_s^2 defined by $C_s^2 = \frac{\partial p / \partial N}{\partial \rho / \partial N}$. The model is said to be classically stable if $C_s^2 \geq 0$ at local critical points[62, 63]. It is important to note that local stability does not imply the classical stability. From cosmological point of view, those points which are locally as well as classically stable are of interest.

A. Interaction A: $Q = \sqrt{\frac{2}{3}} \alpha \rho_m \dot{\phi}$

In this case using dimensionless variables (17) the evolution equations can be converted to the following autonomous system

$$x' = -3x + \frac{\theta}{2} s \sqrt{6} y^2 + \frac{3}{2} \frac{x (2\theta x^2 + \gamma (2z^2 - \theta x^2 - y^2 + 1))}{z^2 + 1} + \theta \alpha (2z^2 - \theta x^2 - y^2 + 1) \quad (23)$$

$$y' = -\frac{1}{2} s \sqrt{6} x y + \frac{3}{2} \frac{y (2\theta x^2 + \gamma (2z^2 - \theta x^2 - y^2 + 1))}{z^2 + 1} \quad (24)$$

$$z' = \frac{3}{4} \frac{z (2\theta x^2 + \gamma (2z^2 - \theta x^2 - y^2 + 1))}{z^2 + 1} \quad (25)$$

$$s' = -\sqrt{6} x s^2 (\Gamma - 1) \quad (26)$$

where prime denotes derivative with respect to $N = \ln a$. It is noted from eqn.(23) that when $\Omega_m = 0$, the last term containing α vanishes *i.e.*, point where $\Omega_m = 0$ is independent of the interaction Q for its

existence and hence it exists in case of uncoupled model also. It can be seen that the above system is invariant under the change of sign $z \rightarrow -z$ and $y \rightarrow -y$. So, we restrict our analysis to the positive values of y and z only.

The adiabatic speed of sound C_s^2 is given by

$$C_s^2 = 1 + \frac{2sy^2}{\left(\sqrt{\frac{2}{3}}\alpha(1 - \theta x^2 - y^2 + 2z^2) - \sqrt{6}\theta x\right)} \quad (27)$$

In what follows we study the phase space analysis of above two categories of potentials separately.

1. **Category I:** Non-exponential form of potential ($\Gamma \neq 1$)

In this category, eqns. (23)-(26) form a closed system of equations. The critical points along with corresponding cosmological parameters are given in table I and the eigenvalues of their corresponding Jacobian matrix are given in table II.

TABLE I: Critical points and corresponding cosmological parameters

Point	x	y	z	s	Existence	Ω_ϕ	ω_ϕ	q
A_1	$\frac{1}{\sqrt{\theta}}$	0	0	0	$\theta > 0$	1	1	2
A_2	$-\frac{1}{\sqrt{\theta}}$	0	0	0	$\theta > 0$	1	1	2
A_3	$\frac{2\alpha\theta}{3(2-\gamma)}$	0	0	0	$\gamma \neq 2$ and $\theta\alpha^2 < \frac{9(2-\gamma)^2}{4}$	$\frac{4\theta\alpha^2}{9(2-\gamma)^2}$	1	$\frac{2\alpha^2\theta}{3(2-\gamma)} + \frac{3}{2}\gamma - 1$
A_4	0	$\sqrt{2z^2+1}$	z	0	Always	$2z^2+1$	-1	-1

TABLE II: Eigenvalues of critical points in table I

Point	E_1	E_2	E_3	E_4	C_s^2
A_1	0	$\frac{3}{2}$	3	$3(2-\gamma) - 2\alpha\sqrt{\theta}$	1
A_2	0	$\frac{3}{2}$	3	$3(2-\gamma) + 2\alpha\sqrt{\theta}$	1
A_3	0	$\frac{4\alpha^2\theta+9\gamma(2-\gamma)}{12(2-\gamma)}$	$\frac{4\alpha^2\theta-9(2-\gamma)^2}{6(2-\gamma)}$	$\frac{4\alpha^2\theta+9\gamma(2-\gamma)}{6(2-\gamma)}$	1
A_4	0	0	-3	-3 γ	stable (limiting)

We now discuss the stability of critical points given in table I separately for quintessence and phantom field.

(i) Quintessence field ($\theta = 1$):

Points A_1 and A_2 correspond to the un-accelerated, dominated by kinetic part of quintessence field ($\Omega_\phi = 1, \Omega_m = 0, q = 2$). A_1 is an unstable node if $3(2-\gamma) > 2\alpha$ and A_2 is an unstable node if $3(2-\gamma) > -2\alpha$, else they behave as saddle points. Point A_3 behaves as a saddle fixed point (since E_2 and E_4 are positive but E_3 is negative in the existence region of this point). Points on a set of critical points A_4 correspond to an accelerated solution ($q = -1$) and since it has two zero eigenvalues and two negative eigenvalues, so linear stability theory is not enough and further investigation is required to decide the stability of this set.

To check the stability of this set of non isolated critical points A_4 , we numerically perturb the solutions around a critical point of the set.

We plot the perturbation plots projected on the x, y, z and s axes separately. From figs.1(a) and 1(b), it is evident that trajectories of perturbed solutions approach $x = 0$ and $s = 0$ respectively as $N \rightarrow \infty$. It seems that trajectories in fig.1(b) are parallel to a horizontal axis but they do converge to $s = 0$, but converge slowly. Indeed we have checked that trajectories actually converge to $s = 0$ as $N \rightarrow \infty$. Furthermore, we note from fig.1(c) that any perturbation of the system near z makes it constant at the perturbed value and it shows that z

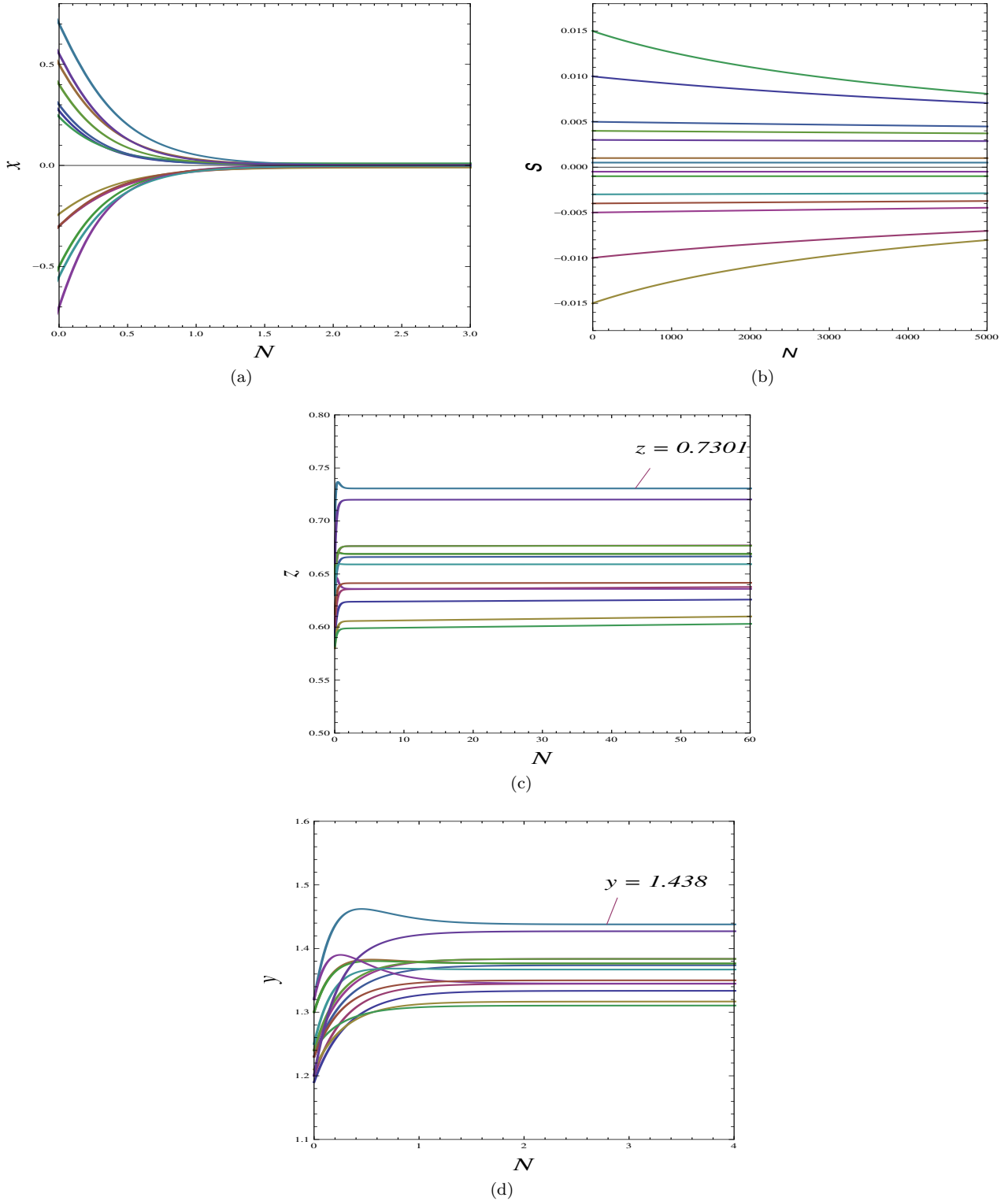


FIG. 1: (a). Projection of perturbation plot of x versus N . (b). Projection of perturbation plot of s versus N . (c). Projection of perturbation plot of z versus N . (d). Projection of perturbation plot of y versus N for $\theta = 1$.

is arbitrary. We can also see from fig.1(d), that for each value of z , where the trajectories approach as $N \rightarrow \infty$, the corresponding trajectories of y also approach the value $\sqrt{2z^2 + 1}$ as $N \rightarrow \infty$. One such trajectory is shown in fig.1(c) where $z = 0.7301$ and $y = \sqrt{2z^2 + 1} = 1.438$ in fig.1(d). From these behaviours of the system near A_4 , we can conclude that A_4 is a late time attractor. It is interesting to see the effect of brane in solution A_4 . This indeed shows role of brane in explaining late time acceleration.

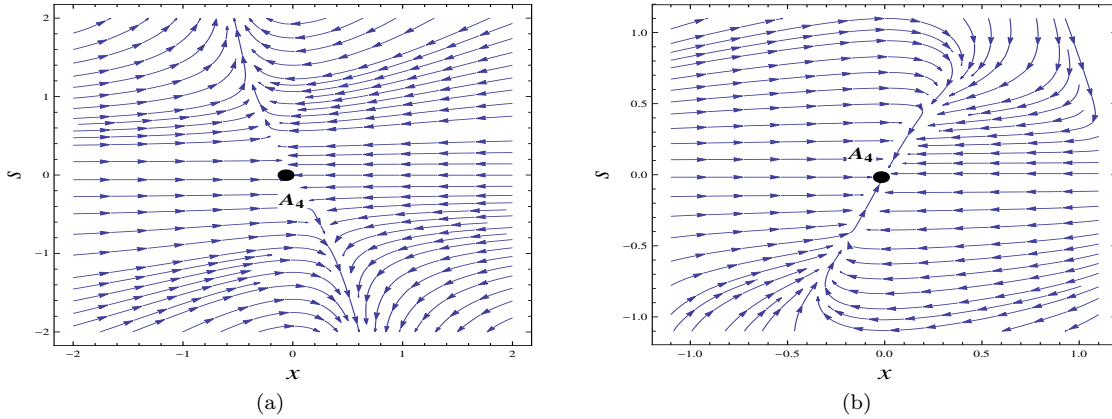


FIG. 2: (a). Projection of the system (23)-(26) on $x - s$ plane for $\theta = -1$. (b). Projection of the system (23)-(26) on $x - s$ plane for $\theta = 1$. Here $\alpha = -0.7$, $\gamma = 1$.

In the phase space of the autonomous system any heteroclinic orbit starts from an unstable critical point (past time attractor) and evolve to a stable critical point (late time attractor) via saddle points.

So, a viable cosmological model must have a past time attractor, saddle points and late time attractors to represent early universe, radiation or matter dominated eras and late time acceleration respectively.

In this case, universe evolves from one of these unstable points A_1 or A_2 and approaches toward the saddle point A_3 and finally settles down towards the attractor set A_4 . Furthermore, the attractor set A_4 is also classically stable and very interesting from cosmological point of view.

(ii) Phantom field ($\theta = -1$):

Critical points A_1 , A_2 do not exist for this case of phantom field. Point A_3 is physically meaningless, since Ω_ϕ is negative. The set of critical points A_4 corresponds to an accelerated solution. Fig.2(a) shows the 2D projection of the system on the $x - s$ plane. We observe that trajectories which initially approach a point $(0,0)$ in $x - s$ plane, ultimately moves away from it. This implies that a set of critical points A_4 is an unstable set unlike the case of a quintessence field which is stable (see figs.2(a) and 2(b)). Thus, non exponential potential do not give any interesting cosmological scenarios for this case.

2. Category II: Exponential form of potential ($\Gamma = 1$)

In this category, s is constant and $V = V_0 \exp(-\lambda\phi)$, so eqs.(23)-(25) form a closed system of equations. Critical points and their cosmological parameters are listed in table III and the eigenvalues of their corresponding Jacobian matrix are given in table IV. In what follows we discuss the stability of critical points for $\theta = 1$ and $\theta = -1$ separately under this potential.

(i) Quintessence field ($\theta = 1$):

Point B_1 is an unstable node if $\alpha < \frac{3(2-\gamma)}{2}$ and $\lambda < \sqrt{6}$, otherwise it is saddle. B_2 is an unstable node if $\alpha < \frac{3(2-\gamma)}{2}$ and $\lambda > -\sqrt{6}$, otherwise it is saddle. Both B_1, B_2 correspond to un-accelerated, quintessence kinetic energy dominated solutions ($q = 2, \Omega_\phi = 1$). Point B_3 corresponds to a scaling solution for $\alpha \neq 0$ and it is a saddle point (since eigenvalue E_2 is negative, whereas E_1 is always positive in its region of existence). Point B_4 corresponds to scalar field dominated point, which can be accelerated if $\lambda^2 < 2$. It is a saddle point since E_1 is positive and E_2 is negative in the region of existence. From figs.3(a) and 3(b) it can be seen that the region of existence of B_5 and region of positivity of its eigenvalue E_3 are disjoint. This numerically confirms that E_3 is negative, but E_1 is always positive. Thus, scaling point B_5 is a saddle point. The instability of B_5 is in contrary with the result in standard GR found in references [33, 54] where this point corresponds to a scaling late time attractor. The set of critical points B_6 demands $\lambda = 0$ for its existence, which means that $V(\phi)$ is constant. It is a normally hyperbolic set. Since the remaining non-zero eigenvalues are all negative, so the set of critical points B_6 is a late time attractor.

In this case we see that universe evolves from one of the unstable points B_1 or B_2 and approaches toward any of the saddle points B_3 , B_4 or B_5 and finally settles down towards the attracting set B_6 . Furthermore, the attractor set B_6 is also classically stable and is very interesting from cosmological point of view.

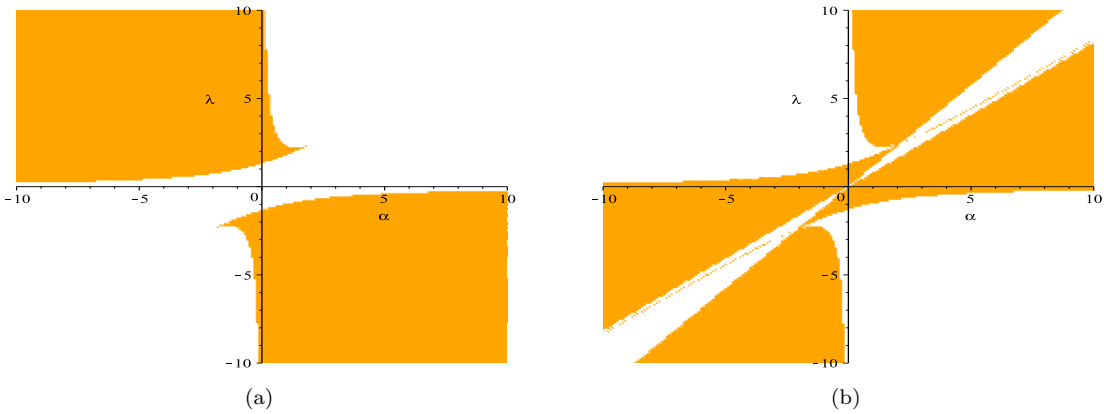
TABLE III: Critical points and their cosmological parameters of system (We have defined: $b = \lambda - \frac{\sqrt{6}}{3}\alpha$)

Point	x	y	z	Existence	Ω_ϕ	ω_ϕ	q
B_1	$\frac{1}{\sqrt{\theta}}$	0	0	$\theta > 0$	1	1	2
B_2	$-\frac{1}{\sqrt{\theta}}$	0	0	$\theta > 0$	1	1	2
B_3	$\frac{2\theta\alpha}{3(2-\gamma)}$	0	0	$\gamma \neq 2$ $\theta\alpha^2 < \frac{9(2-\gamma)^2}{4}$	$\frac{4\theta\alpha^2}{9(2-\gamma)^2}$	1	$\frac{2\theta\alpha^2}{3(2-\gamma)} + \frac{3}{2}\gamma - 1$
B_4	$\frac{\theta\lambda}{\sqrt{6}}$	$\sqrt{1 - \frac{\theta\lambda^2}{6}}$	0	$\theta\lambda^2 < 6$	1	$\frac{\theta\lambda^2}{3}$	$\frac{\theta\lambda^2}{2} - 1$
B_5	$\frac{\gamma\sqrt{6}}{2b}$	$\frac{\sqrt{9\theta\gamma(2-\gamma)-2\sqrt{6}\alpha b}}{\sqrt{6}b}$	0	$9\theta\gamma(2-\gamma) > 2\sqrt{6}\alpha b$ $9\gamma^2 + 9\theta\gamma(2-\gamma) < 2b(\sqrt{6}\alpha + 3b)$	$\frac{9\gamma(\gamma+\theta(2-\gamma))-2\sqrt{6}\alpha b}{6b^2}$	$\frac{9\theta\gamma^2+\sqrt{6}\alpha b-9\theta\gamma}{-\sqrt{6}\alpha b+9\theta\gamma}$	$\frac{\sqrt{6}\gamma\alpha+3\gamma b-2b}{2b}$
B_6	0	$\sqrt{2z^2+1}$	z	Always	$2z^2+1$	-1	-1

TABLE IV: Eigenvalues of critical points in table III

Point	E_1	E_2	E_3	C_s^2
B_1	$3 - \frac{\sqrt{6\theta}}{2}\lambda$	$\frac{3}{2}$	$3(2-\gamma) - 2\alpha\sqrt{\theta}$	1
B_2	$3 + \frac{\sqrt{6\theta}}{2}\lambda$	$\frac{3}{2}$	$3(2-\gamma) + 2\alpha\sqrt{\theta}$	1
B_3	$\frac{1}{12} \frac{4\alpha^2\theta+9\gamma(2-\gamma)}{(2-\gamma)}$	$\frac{1}{6} \frac{4\alpha^2\theta-9(2-\gamma)^2}{(2-\gamma)}$	$\frac{1}{6} \frac{-2\sqrt{6}\lambda\alpha\theta+4\alpha^2\theta+9\gamma(2-\gamma)}{(2-\gamma)}$	1
B_4	$\frac{\theta\lambda^2}{4}$	$\frac{\theta\lambda^2}{2} - 3$	$-\frac{1}{3}\sqrt{6}\alpha\lambda\theta + \theta\lambda^2 - 3\gamma$	$\frac{\theta\lambda^2}{3} - 1$
B_5	$\frac{\gamma(3b+\sqrt{6}\alpha)}{4b}$	μ_+	μ_-	$-1 + \frac{9\theta\gamma^2}{9\theta\gamma-\sqrt{6}\alpha b}$
B_6	0	-3	-3γ	stable (limiting)

$$\text{where, } \mu_{\pm} = -\frac{(3b(2-\gamma)-\gamma\sqrt{6}\alpha)}{4b} \left[1 \pm \sqrt{1 - \frac{24(3\gamma(2-\gamma)-\frac{2}{3}\sqrt{6}\theta\alpha b)(\theta(\frac{\alpha\sqrt{6}b}{3}+b^2)-3\gamma)}{(3b(2-\gamma)-\gamma\sqrt{6}\alpha)^2}} \right]$$

FIG. 3: (a). Stability region of B_5 . (b). Region of positivity of eigenvalue E_3 with $\theta = 1, \gamma = 1$ for B_5 .

The behaviour of deceleration parameter q for the case of $\Gamma = 1$ is given in fig.4(a). The universe undergoes transition from decelerated phase to an accelerated phase around $N = -0.44$ (equivalent to a redshift of 0.55). This indeed matches with the observation [46]. Finally universe settles down with an accelerated expansion ($q = -1$). Also crossing of phantom divide is possible as shown in fig.4(b) for quintessence field. A similar behaviour can be observed for the case of $\Gamma \neq 1$ also. The crossing of phantom divide line can also be understood analytically. For $\omega_\phi > -1$ and $\gamma = 1$, we see from eqn.(13) that $1+\omega_{\text{eff}}$ can assume positive as well

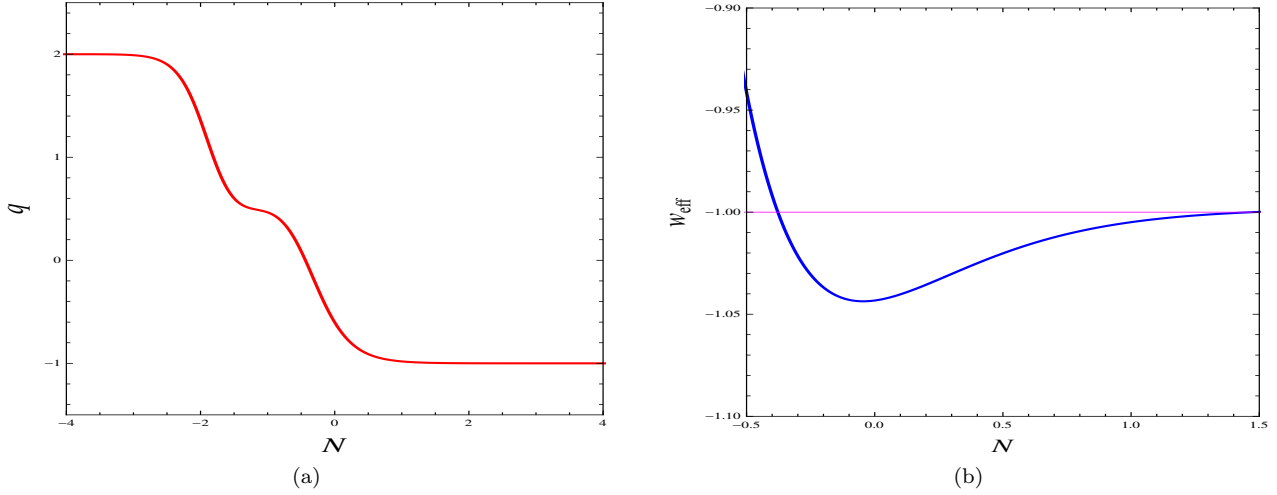


FIG. 4: (a). Plot of q versus N . (b). Plot of ω_{eff} vs N for $\theta = 1$, for $\Gamma = 1$ with $\alpha = -0.7$, $\gamma = 1$.

as negative values. Hence ω_{eff} can pass through -1.

(ii) Phantom field ($\theta = -1$):

Critical points B_1, B_2 do not exist in this case. Point B_3 is physically meaningless since Ω_ϕ is negative. Point B_4 corresponds to an accelerated phantom field dominated solution ($\Omega_\phi = 1, q = -\frac{\lambda^2}{2} - 1$). It is a late time attractor if $\alpha < \frac{\sqrt{6}}{2\lambda}(\lambda^2 + 3\gamma)$. However this point is not classically stable. Scaling solution B_5 is stable for a narrow range of parameters. Fig.5(a) shows the region of stability and the complicated conditions for stability is confirmed numerically. It can be seen that, if we numerically put $\alpha = 1.8, \lambda = 0.7, \gamma = 0.5$, we obtain $E_1 = -0.34, E_2 = -3.67, E_3 = -0.008, C_s^2 = 1.03, q = -1.68, \Omega_\phi = 0.64$ within the region of existence of B_5 . Thus we get a late time accelerated scaling attractor in this case. Fig. 5(b) shows the projection of the system on $y - z$ plane. This is indeed an interesting point since this point is not obtained in case of corresponding uncoupled DGP model [44]. For the non isolated set of critical points B_6 , we plot a projection of a system on the $x - y$ plane (fig.6). We observe that a point (0,1) which lies on $x - y$ plane is unstable and hence B_6 is unstable. In this case universe starts from an unknown point and finally settles down to point B_5 .

The behaviour of deceleration parameter q for the case of $\Gamma = 1$ is given in fig.7(a). The universe is always in accelerated phase. Also crossing of phantom divide is not possible as shown in fig.7(b). A similar behaviour can be observed for the case of $\Gamma \neq 1$ also. This also can be understood analytically, since for $\omega_\phi < -1$ and $\gamma = 1$, the numerator of eqn.(13) is always positive. In fig.7(b), ω_{eff} seems to diverge. Actually no pathology is associated to the model and this divergence is associated with effective behaviour. This happens because Ω_{eff} evolve from either positive to negative values or vice versa. So, $\Omega_{\text{eff}} = 0$ at some values of N , which leads to the breakdown of the effective behaviour. This sort of behaviour is also obtained in [27, 30].

B. Interaction B: $Q = \beta \dot{\rho}_\phi$

The autonomous system of equation for this interaction is given by

$$x' = \frac{3x}{(\beta - 1)} + \theta \frac{1}{2} s \sqrt{6} y^2 + \frac{3}{2} \frac{x(2\theta x^2 + \gamma(2z^2 - \theta x^2 - y^2 + 1))}{z^2 + 1} \quad (28)$$

$$y' = -\frac{1}{2} s \sqrt{6} x y + \frac{3}{2} \frac{y(2\theta x^2 + \gamma(2z^2 - \theta x^2 - y^2 + 1))}{z^2 + 1} \quad (29)$$

$$z' = \frac{3}{4} \frac{z(2\theta x^2 + \gamma(2z^2 - \theta x^2 - y^2 + 1))}{z^2 + 1} \quad (30)$$

$$s' = -\sqrt{6} x s^2 (\Gamma - 1) \quad (31)$$

It is noted when $x = 0$, the first term on the right hand side of eq.(28) containing β vanishes. So, point where $x = 0$ is independent of the interaction Q and hence exists in uncoupled model also. It can also be seen that the system is invariant under the change of sign $y \rightarrow -y$ and $z \rightarrow -z$, so we restrict our analysis to the positive values of y and z .

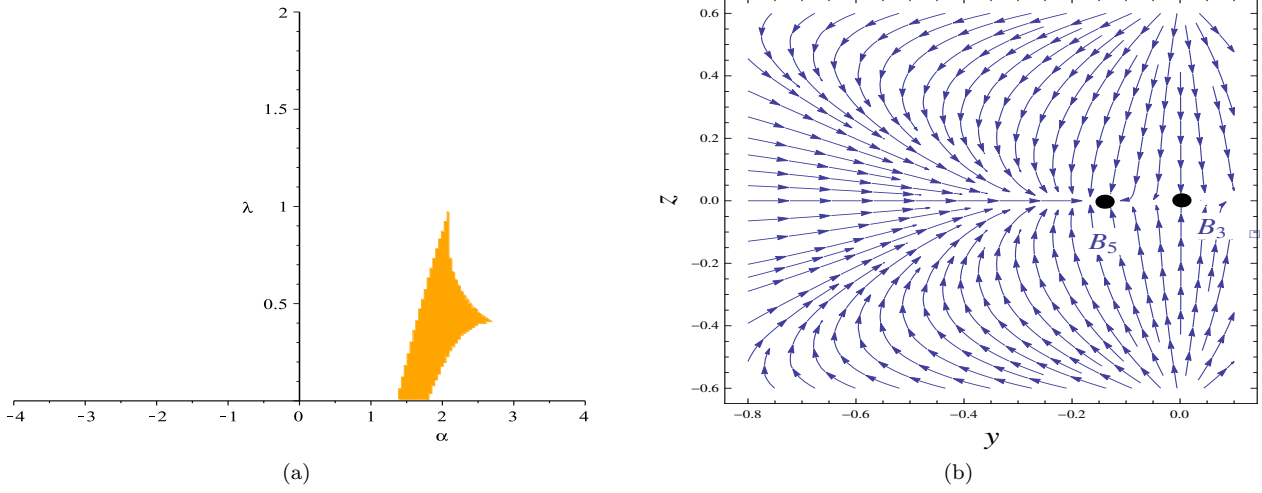


FIG. 5: (a). Region of stability of B_5 . (b). $y - z$ plane projection of the system (23)-(25) for $\theta = -1$ with $\alpha = 1.8$, $\gamma = 0.5$.

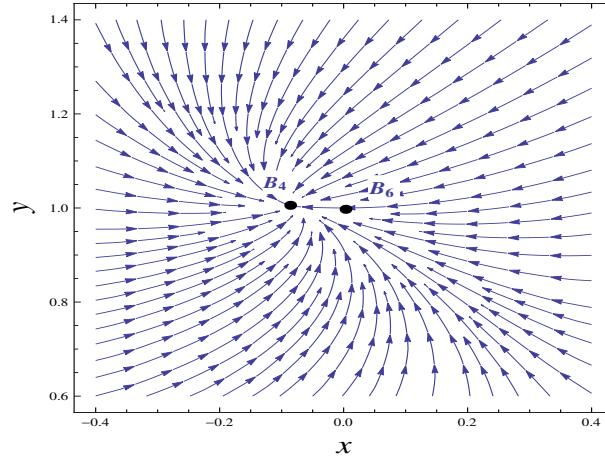


FIG. 6: $x - y$ plane projection of the system (23)-(25) for $\theta = -1$.

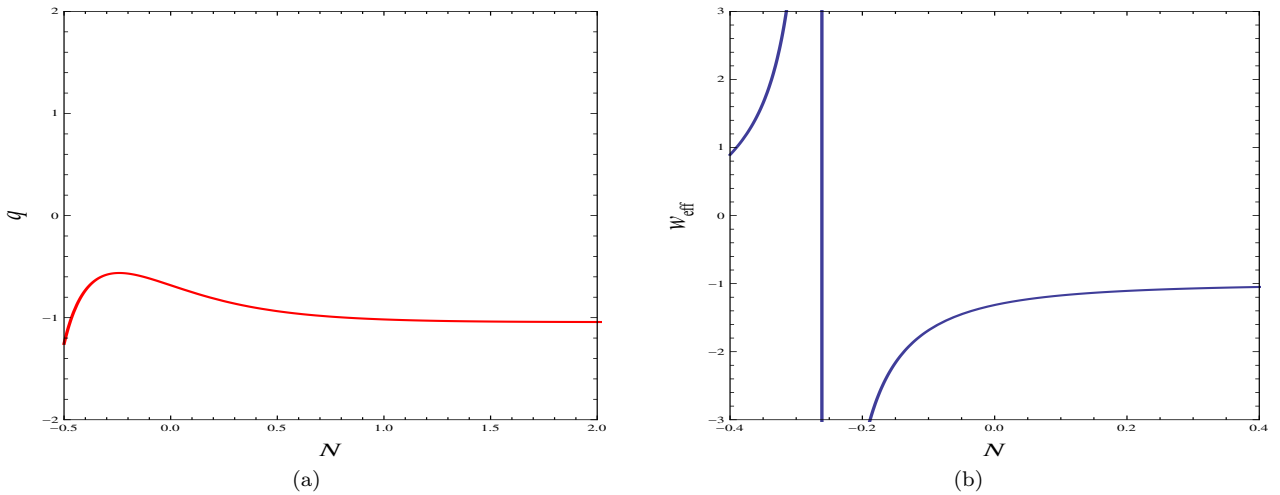


FIG. 7: (a). Plot of q versus N (b). Plot of ω_{eff} vs N for $\theta = -1$, $\Gamma = 1$ with $\alpha = -0.7$, $\gamma = 1$.

The adiabatic speed of sound C_s^2 is given by

$$1 + \frac{2\theta(\beta - 1)s y^2}{\sqrt{6}x} \quad (32)$$

As before, in what follows we study the phase space analysis for the two categories of potentials.

1. **Category I: Non-exponential form of potential** ($\Gamma \neq 1$)

In this category eqs.(28)-(31) form a closed system of equations. The critical points and their cosmological parameters are listed in table V and the eigenvalues of their corresponding Jacobian matrix are given in table VI. Like previous case, we discuss the stability of critical points for the two fields separately.

TABLE V: Critical points and their cosmological parameters of system. We have defined: $\xi_{\pm} = \pm \sqrt{-\frac{(\beta\gamma + (2-\gamma))}{\theta(\beta-1)(2-\gamma)}}$

Point	x	y	z	s	Existence	Ω_{ϕ}	ω_{ϕ}	q
C_1	0	0	0	s	Always	0	1	$-1 + \frac{3\gamma}{2}$
C_2	ξ_+	0	0	0	$0 < \theta\xi_+^2 < 1$ $\beta \neq 1, \gamma \neq 2$	$\theta\xi_+^2$	1	$-\frac{\beta+2}{\beta-1}$
C_3	ξ_-	0	0	0	$0 < \theta\xi_-^2 < 1$ $\beta \neq 1, \gamma \neq 2$	$\theta\xi_-^2$	1	$-\frac{\beta+2}{\beta-1}$
C_4	0	$\sqrt{2z^2 + 1}$	z	0	Always	$2z^2 + 1$	-1	-1

TABLE VI: Eigenvalues of critical points in table V

Point	E_1	E_2	E_3	E_4	C_s^2
C_1	$\frac{3}{\beta-1} + \frac{3\gamma}{2}$	$\frac{3\gamma}{2}$	$\frac{3\gamma}{4}$	0	stable (limiting)
C_2	$3\theta(2-\gamma)\xi_+^2$	$-\frac{3}{\beta-1}$	$-\frac{3}{2(\beta-1)}$	0	1
C_3	$3\theta(2-\gamma)\xi_-^2$	$-\frac{3}{\beta-1}$	$-\frac{3}{2(\beta-1)}$	0	1
C_4	-3γ	$\frac{3}{\beta-1}$	0	0	undefined

(i) Quintessence field ($\theta = 1$):

C_1 corresponds to an accelerated matter dominated universe ($\Omega_m = 1$) for $\gamma < \frac{2}{3}$. It is an unstable node for $\frac{\gamma}{2} > \frac{1}{1-\beta}$ otherwise it behaves as a saddle point. Scaling solutions C_2 and C_3 are unstable nodes for $\beta < 1$ else they behave as saddle points. Set of critical points C_4 corresponds to an accelerated solution ($q = -1$). Since two of its eigenvalues are zero and the other two are negative provided $\beta < 1$, (it behaves as a saddle point for $\beta > 1$), so linear stability theory is not enough and further investigation is required. To check the stability of this non isolated set, we numerically perturb the solutions around the critical point. We again plot the projections plots on x, y, z and s separately. Like previous case, from figs.8(a)-8(d), it is evident that the non isolated set of critical points C_4 is a late time attractor.

In this case, universe evolves from one of these unstable points C_2 or C_3 and approaches toward the saddle point C_1 and finally settles down towards the attractor set C_4 .

(ii) Phantom field ($\theta = -1$):

Critical points C_2, C_3 do not exist for phantom field. Critical point C_1 is unstable node for $\frac{1}{(1-\beta)} < \frac{\gamma}{2}$, otherwise it behaves as saddle point. The set of critical points C_4 corresponds to an accelerated solution. Since its corresponding Jacobian matrix contains two zero and two negative eigenvalues, further investigation is required. As in case of interaction **A**, we plot a 2D projection of the system on the $x - s$ plane and we observe that trajectories which initially approach a point $(0,0)$ which lies on set C_4 , ultimately diverge away from it. This implies that a set of points C_4 is an unstable set. Thus we do not get any interesting cosmological scenario in this case.

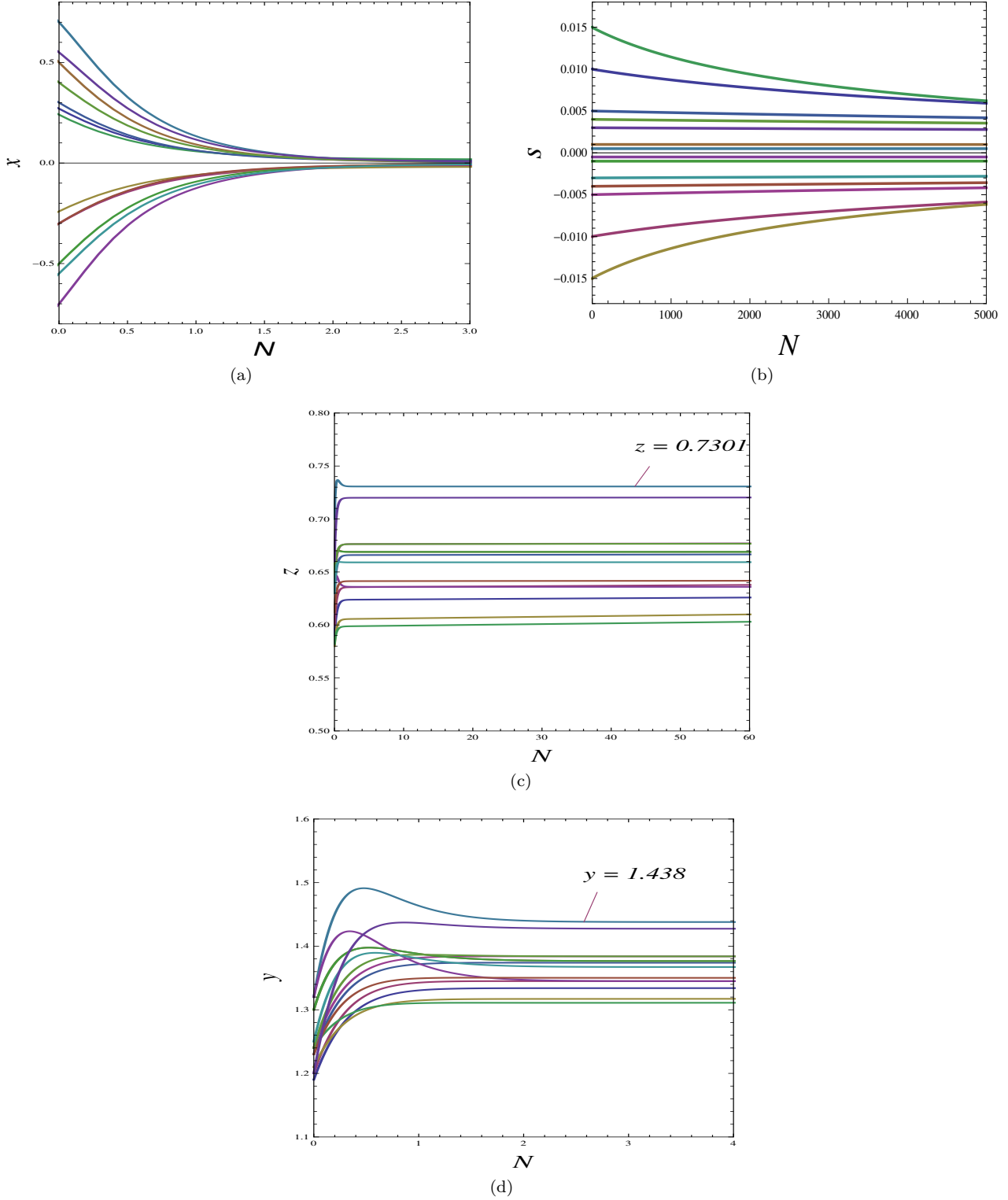


FIG. 8: (a). Projection of perturbation plot of x versus N . (b). Projection of perturbation plot of s versus N . (c). Projection of perturbation plot of z versus N . (d). Projection of perturbation plot of y versus N for $\theta = 1$.

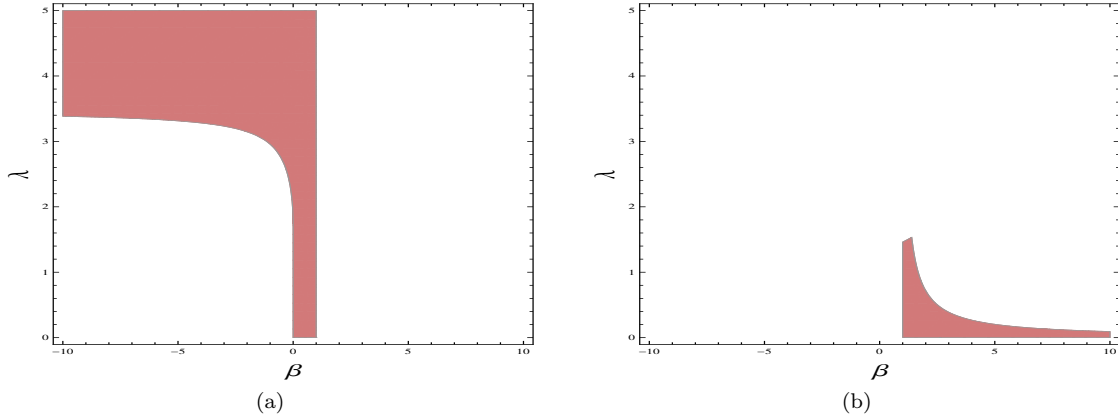
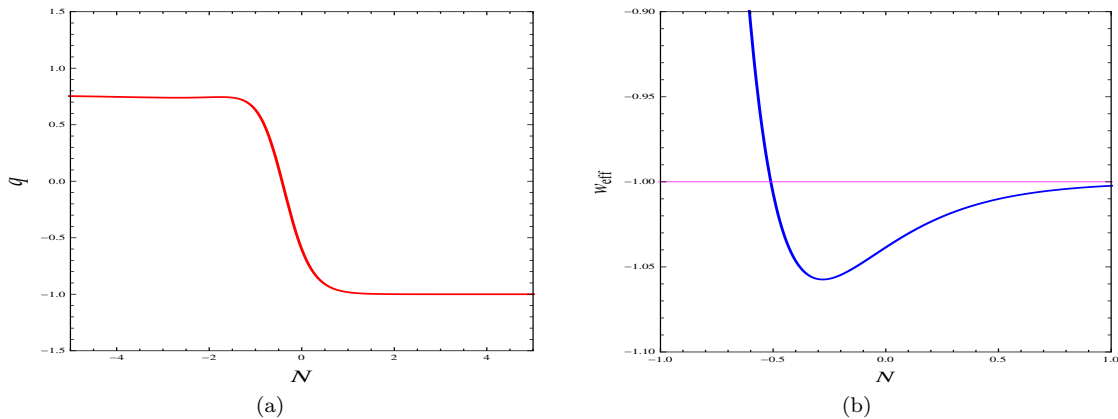
2. Category II: Exponential form of potential ($\Gamma = 1$)

In this category, s is constant and $V = V_0 \exp(-\lambda\phi)$, so eqs.(28)-(30) form a closed system of equations. Critical points and corresponding cosmological parameters are listed in table VII and the eigenvalues of their corresponding Jacobian matrix are given in table VIII. As before, we discuss the stability of critical points for two scalar fields separately.

TABLE VII: Critical points and cosmological parameters. We have defined: $\xi_{\pm} = \pm \sqrt{-\frac{(\beta\gamma+(2-\gamma))}{\theta(\beta-1)(2-\gamma)}}$

Point	x	y	z	Existence	Ω_{ϕ}	ω_{ϕ}	q
D_1	0	0	0	Always	0	1	$-1 + \frac{3\gamma}{2}$
D_2	ξ_+	0	0	$0 < \theta\xi_+^2 < 1$	$\theta\xi_+^2$	1	$-\frac{\beta+2}{\beta-1}$
D_3	ξ_-	0	0	$0 < \theta\xi_-^2 < 1$	$\theta\xi_-^2$	1	$-\frac{\beta+2}{\beta-1}$
D_4	0	$\sqrt{2z^2+1}$	z	Always	$2z^2+1$	-1	-1
D_5	x_5	y_5	0	$\theta x_5^2 + y_5^2 < 1$	$x_5^2 + y_5^2$	$\frac{x_5^2 - y_5^2}{x_5^2 + y_5^2}$	$\frac{1}{16\lambda^2(\beta-1)^2} \left[\{\lambda^2(\beta-1) + 10\beta + 2\delta - 7\}^2 - 27 + 3\delta^2 - (10\beta + 2\delta - 7)^2 \right]$

$$\begin{aligned}
 & \text{For quintessence field,} \\
 x_5 &= \frac{\sqrt{6}(\lambda^2(\beta-1)-3+\delta)}{12\lambda(\beta-1)}, y_5 = \frac{\sqrt{-3(\delta^2+6\beta(\lambda^2(\beta-1)+3)-18(\beta+1)+(\lambda^2(\beta-1)+3)\delta)}}{6\lambda(\beta-1)}, \delta = \sqrt{\lambda^2(\beta-1)(\lambda^2(\beta-1)+6(1-2\beta))+9} \\
 & \text{For phantom field,} \\
 x_5 &= \frac{\sqrt{6}(-\lambda^2(\beta-1)-3+\delta)}{12\lambda(\beta-1)}, y_5 = \frac{\sqrt{3(\delta^2-6\beta(\lambda^2(\beta-1)-3)-18(\beta+1)+(\lambda^2(\beta-1)-3)\delta)}}{6\lambda(\beta-1)}, \delta = \sqrt{\lambda^2(\beta-1)(\lambda^2(\beta-1)-6(1-2\beta))+9}
 \end{aligned}$$


 FIG. 9: (a). Existence region of point D_5 . (b). Region for negativity of one eigenvalue η_1 with $\theta = 1$.

 FIG. 10: (a). Plot of q versus N . (b). Plot of ω_{eff} vs N for $\theta = 1$, $\Gamma = 1$ with $\beta = -0.7$, $\gamma = 1$.

(i) Quintessence field ($\theta = 1$):

Point D_1 corresponds to an accelerated matter dominated solution ($\Omega_m = 1$) for $\gamma < \frac{2}{3}$. It is an unstable node for $\frac{1}{1-\beta} < \frac{\gamma}{2}$, otherwise it is a saddle point. Scaling solutions D_2 and D_3 are unstable nodes for $\beta < 1$ and are saddle points for $\beta > 1$. A set of non isolated critical points D_4 demands $\lambda = 0$ for its existence (i.e.,

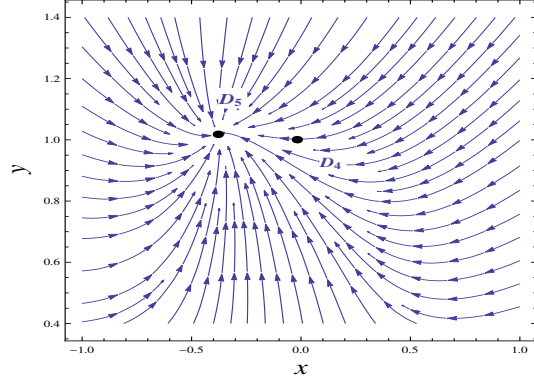


FIG. 11: $x - y$ plane projection of the system (28)-(30) for $\theta = -1$. It seems that point D_5 is stable but actually not stable.

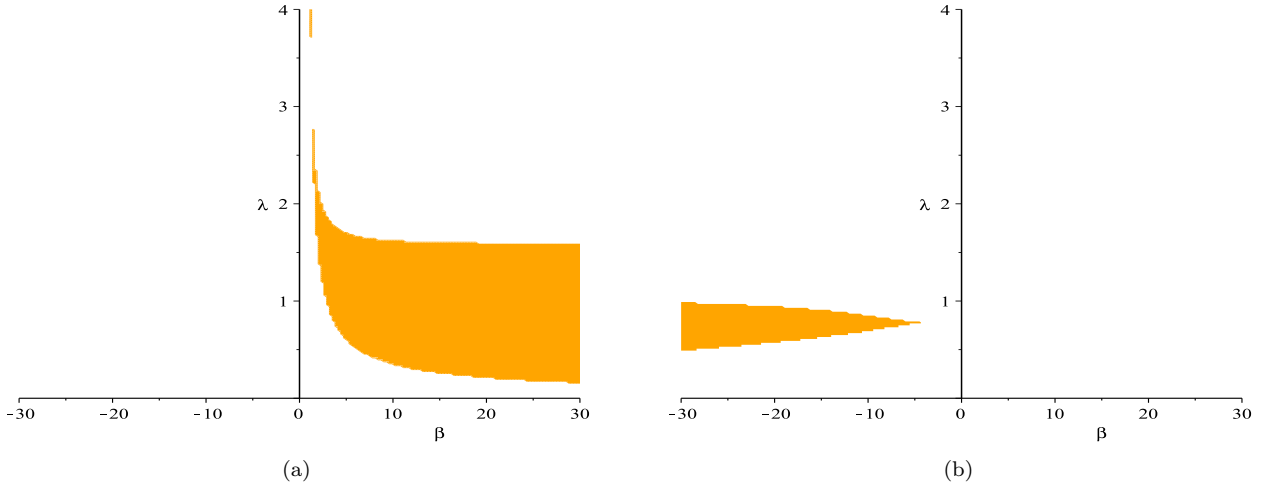


FIG. 12: (a). Existence region of point D_5 . (b). Region for negativity of one eigenvalue η_+ with $\theta = -1$.

$V(\phi)$ is constant). Since this set is a normally hyperbolic set, so this non isolated set of critical points is a late time attractor if $\beta < 1$, else it will be saddle. For point D_5 , since eigenvalues are too complicated to determine stability of the point analytically, we consider the case of dust matter only ($\gamma = 1$). We plot a region of existence of the point and region for negativity of one of its eigenvalues as shown in figs.9(a) and 9(b) respectively. We found that these two regions are disjoint, which implies that the eigenvalue must be positive for that point to exist. Hence, this point is unstable, for $\gamma = 1$. The instability of point D_5 is in contrary with the result in standard GR found in ref [38], where this point corresponds to a scaling late time attractor.

In this case, universe evolves from one of these unstable points D_2 or D_3 and approaches toward the saddle point D_1 or D_5 and finally settles down towards the attractor set D_4 .

The behaviour of deceleration parameter q for the case of $\Gamma = 1$ is given in fig.10(a). The universe undergoes transition from decelerated phase to an accelerated phase around $N = -0.44$ (equivalent to a redshift 0.55) which match with the observation [46]. Finally the universe settles down to an accelerated expansion ($q = -1$). Also crossing of phantom divide is possible as shown in fig.10(b) for quintessence field. A similar behaviour can be observed for the case of $\Gamma \neq 1$ also. In this case also the crossing of phantom divide line can be understood analytically as in case of interaction **A**.

(ii) Phantom field ($\theta = -1$):

Critical points D_2, D_3 do not exist for phantom field. Critical point D_1 corresponds to an accelerated matter dominated phase for $\gamma < \frac{2}{3}$. It is unstable node if $\frac{1}{1-\beta} < \frac{7}{2}$, else it is a saddle point. A set of non isolated critical points D_4 corresponds to an accelerated solution. Again, since its Jacobian matrix contains two negative and one zero eigenvalues, further investigation is required. We plot the projection of the system on $x - y$ plane and from (fig.11) we observe that point $(0, 1)$ which lies on the set D_4 is not stable. Therefore, the set D_4 is not a stable set. For critical point D_5 since it is too complicated to determine its stability, we focus only in the case of dust matter ($\gamma = 1$). As before, we plot the existence region of a point (fig.12(a)) and the

TABLE VIII: Eigenvalues of critical points in table VII

Point	E_1	E_2	E_3	C_s^2
D_1	$\frac{3}{\beta-1} + \frac{3\gamma}{2}$	$\frac{3\gamma}{2}$	$\frac{3\gamma}{4}$	undefined(stable limiting)
D_2	$3\theta(2-\gamma)\xi_+^2$	$-\frac{3}{\beta-1}$	$-\frac{3}{2(\beta-1)}$	1
D_3	$3\theta(2-\gamma)\xi_-^2$	$-\frac{3}{\beta-1}$	$-\frac{3}{2(\beta-1)}$	1
D_4	-3γ	$\frac{3}{\beta-1}$	0	undefined
D_5	η_1	η_+	η_-	Given below

For point D_5 (quintessence field)

$$\eta_1 = \frac{\beta^2\lambda^4 - 2\beta\lambda^4 + 36\beta^2\lambda^2 + 4\beta\delta\lambda^2 + \lambda^4 - 66\lambda^2\beta - 4\delta\lambda^2 + 3\delta^2 + 30\lambda^2 - 27}{32\lambda^2(\beta-1)^2}$$

$$\eta_{\pm} = \frac{1}{64\lambda^2(\beta-1)^2} [192\beta^2\lambda^2 + 24\beta\delta\lambda^2 - 216\lambda^2\beta - 24\delta\lambda^2 + 24\delta^2 + 24\lambda^2 - 216 \pm (9\beta^4\lambda^8 - 36\beta^3\lambda^8 + 72\beta^4\lambda^6 + 36\beta^3\delta\lambda^6 + 54\beta^2\lambda^8 - 144\beta^3\lambda^6 - 108\beta^2\delta\lambda^6 - 36\beta\lambda^8 - 240\beta^3\delta\lambda^4 - 10\beta^2\delta^2\lambda^4 + 108\beta\delta\lambda^6 + 9\lambda^8 + 432\beta^3\lambda^4 + 624\beta^2\delta\lambda^4 + 20\beta\delta^2\lambda^4 + 144\beta\lambda^6 - 36\delta\lambda^6 + 72\beta^2\delta^2\lambda^2 - 882\beta^2\lambda^4 - 28\beta\delta^3\lambda^2 - 528\beta\delta\lambda^4 - 10\delta^2\lambda^4 - 72\lambda^6 - 864\beta^3\lambda^2 - 192\beta\delta^2\lambda^2 + 468\beta\lambda^4 + 28\delta^3\lambda^2 + 144\delta\lambda^4 + 1080\beta^2\lambda^2 + 828\beta\delta\lambda^2 + 9\delta^4 + 120\delta^2\lambda^2 - 18\lambda^4 - 864\lambda^2\beta - 828\delta\lambda^2 - 1296\beta^2 - 162\delta^2 + 648\lambda^2 + 1296\beta + 729)^{\frac{1}{2}}]$$

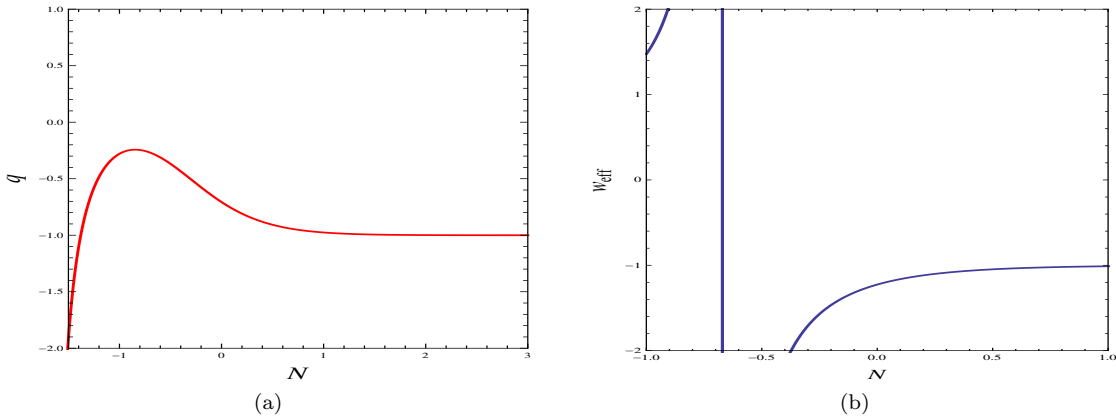
$$C_s^2 = -\frac{6\beta^2\lambda^2 + \beta\delta\lambda^2 - 9\lambda^2\beta - \delta\lambda^2 + \delta^2 + 3\lambda^2 - 9}{3(\lambda^2\beta - \lambda^2 + \delta - 3)}$$

For point D_5 (phantom field)

$$\eta_1 = -\frac{\beta^2\lambda^4 - 2\beta\lambda^4 - 36\beta^2\lambda^2 + \lambda^4 + 66\beta\lambda^2 + 3\delta^2 - 30\lambda^2 - 12\delta - 27}{32\lambda^2(\beta-1)^2}$$

$$\eta_{\pm} = \frac{1}{64\lambda^2(\beta-1)^2} [192\beta^2\lambda^2 - 8\beta\delta\lambda^2 - 216\lambda^2\beta + 8\delta\lambda^2 - 24\delta^2 + 24\lambda^2 + 96\delta + 216 \pm 4(9\beta^4\lambda^8 - 36\beta^3\lambda^8 - 72\beta^4\lambda^6 - 12\beta^3\delta\lambda^6 + 54\beta^2\lambda^8 + 144\beta^3\lambda^6 + 36\beta^2\delta\lambda^6 - 36\beta\lambda^8 - 336\beta^3\delta\lambda^4 + 86\beta^2\delta^2\lambda^4 - 36\beta\delta\lambda^6 + 9\lambda^8 + 432\beta^3\lambda^4 + 648\beta^2\delta\lambda^4 - 172\beta\delta^2\lambda^4 - 144\beta\lambda^6 + 12\delta\lambda^6 - 72\beta^2\delta^2\lambda^2 - 882\beta^2\lambda^4 + 52\beta\delta^3\lambda^2 - 288\beta\delta\lambda^4 + 86\delta^2\lambda^4 + 72\lambda^6 + 864\beta^3\lambda^2 + 288\beta^2\delta\lambda^2 - 144\beta\delta^2\lambda^2 + 468\beta\lambda^4 - 52\delta^3\lambda^2 - 24\delta\lambda^4 - 1080\beta^2\lambda^2 - 1044\beta\delta\lambda^2 + 9\delta^4 + 216\delta^2\lambda^2 - 18\lambda^4 + 864\beta\lambda^2 - 72\delta^3 + 756\delta\lambda^2 - 1296\beta^2 - 18\delta^2 - 648\lambda^2 + 1296\beta + 648\delta + 729)^{\frac{1}{2}}]$$

$$C_s^2 = -\frac{6\beta^2\lambda^2 - \beta\delta\lambda^2 - 9\lambda^2\beta + \delta\lambda^2 - \delta^2 + 3\lambda^2 + 6\delta + 9}{3(\lambda^2\beta - \lambda^2 - \delta + 3)}$$

FIG. 13: (a). Plot of q versus N . (b). Plot of ω_{eff} vs N for $\theta = -1$, $\Gamma = 1$ with $\beta = -0.7$, $\gamma = 1$.

region of negativity of one of its eigenvalue (fig.12(b)). It is observed that these two regions are disjoint which implies that the point is not stable.

In contrast to interaction **A**, we could not extract any late time accelerated scaling attractors in this case. However, for D_5 , $\gamma \neq 1$ may give some interesting solution.

The behaviour of deceleration parameter q for the case of $\Gamma = 1$ is given in fig.13(a). The universe is always in accelerated phase in this case. Also crossing of phantom divide is not possible as shown in fig.13(b). As in case of interaction **A**, there is a breakdown due to the effective behaviour and no pathology is associated with

the model.

IV. CONCLUDING REMARKS

The present work deals with the dynamical system analysis of interacting DE in flat DGP model. The source of DE is taken to be scalar field (quintessence/phantom) and two specific interactions are considered for stability of critical points. Further the stability of critical points are examined for two categories of potentials (exponential and non exponential). The potential is classified in two categories as investigation for these two categories gives complete possible set of choices. For each interaction, we have studied four sub-cases. Performing a detailed stability analysis for each category of potentials for two types of scalar fields we have extracted late time attractors for each interaction along with all important cosmological parameters. Finally in order to predict ultimate fate of evolution, we have also examined classical stability of each critical point for different cases. In what follows we summarise our main results.

While in interaction **A**, there is no matter dominated phase for late time attractors, we do get matter dominated phase for interaction **B**.

For interaction **A** and non exponential potential we get late time accelerated attractor A_4 for quintessence field only. The phantom field in this case does not give any physically interesting result. However for exponential potential, phantom field yields a late time accelerated scaling solution B_5 . Further, this solution is also classically stable. This is very interesting case from cosmological point of view. Moreover, exponential potential also admits in this case late time accelerated attractor B_6 for quintessence field. This result is in contrast to standard cosmology where interacting quintessence only admits late time accelerated scaling solution.

For quintessence field, the interaction **B** gives similar results for both categories of potentials. Phantom field does not give any interesting cosmological solution for both categories of potentials in interaction **B**. It may be noted that due to complicated calculations in the phantom field for the exponential potential, we have examined the point D_5 for $\gamma = 1$ only. So the possibility of having late time accelerated scaling attractor in this case cannot be ruled out for $\gamma \neq 1$. It will be interesting to choose γ in such a way that it gives late time accelerated scaling solution in this interaction also. We leave it for our future work.

Acknowledgement

The authors wish to thank the anonymous referees for helpful suggestions which lead to further improvement of this work.

-
- [1] S. J. Perlmutter *et al*, *Astrophys. J.* **517**, 565 (1999).
 - [2] D. N. Spergel *et al*, *Astrophys J. Suppl.* **148**,175 (2003).
 - [3] A. G. Riess *et al*, *Astrophys. J.* **607**, 665 (2004).
 - [4] P. A. R. Ade *et al* (Planck Collaboration) *Astron Astrophys* **571**, A16 (2014).
 - [5] S.M. Carroll, *Living Rev.Rel.* **4**, 1 (2001).[arXiv:astro-ph/0004075].
 - [6] P. Peebles, P. Ratra, *Rev.Mod.Phys.* **75** 559-606 (2003). [arXiv:astro-ph/0207347]
 - [7] A. R. Liddle, D. H. Lyth, *Cosmological inflation and Large Scale Structure*. Cambridge University Press, Cambridge, England, (2003).
 - [8] J. Magana, T. Matos, *J. Phys. Conf. Ser.* **378**, 012012 (2012).
 - [9] E.V. Linder, *Gen. Rel. Grav.* **40**, 329 (2008). [arxiv:704.2064]
 - [10] C. Armendariz-Picon, V.F. Mukhanov, P.J. Steinhardt, *Phys. Rev. D* **63** 103510 (2001). [arXiv:astro-ph/0006373]
 - [11] R.R. Caldwell, *Phys. Lett. B* **545** 23-29 (2002). [arXiv:astro-ph/9908168]
 - [12] E.J. Copeland, M. Sami, S. Tsujikawa, *Int. J. Modern Phys. D* **15**, 1753 (2006).
 - [13] K. Bamba, S. Capozziello, S. Nojiri, S. D. Odintsov, *Astrophys. Space Sci.* **342** 155-228 (2012).
 - [14] J. Ellis, S. Kalara, K. A. Olive and C. Wetterich, *Phys. Lett. B* **228**, 264 (1989).
 - [15] C. Wetterich, *Astron. Astrophys.* **301**, 321 (1995).
 - [16] L. Amendola, *Phys. Rev. D* **60** 043501 (1999). [arxiv:astro-ph/9904120]
 - [17] Z. K. Guo and Y. Z. Zhang, *Phys. Rev. D* **71**, 023501 (2005).[arXiv:astro-ph/0411524]
 - [18] S. Nojiri, S. D. Odintsov and S. Tsujikawa, *Phys. Rev. D* **71**, 063004 (2005). [arXiv:hep-th/0501025].
 - [19] R. Maartens, *Living Rev. Relativ.* **7**, 7 (2004).
 - [20] G. R. Dvali, G. Gabadadze, M. Porrati, *Phys.Lett. B* **485**,208 (2000).
 - [21] C. Deffayet, *Phys Lett. B* **502**, 199 (2001).
 - [22] J. Dutta, S. Chakraborty and M. Ansari, *Int. J. Theor. Phys.* **49**, 2680 (2010) [arXiv:1006.2206 [gr-qc]].
 - [23] J. Dutta, S. Chakraborty and M. Ansari, *Mod. Phys. Lett. A* **25**, 3069 (2010) [arXiv:1005.5321 [gr-qc]].
 - [24] J. Dutta and S. Chakraborty, *Int. J. Theor. Phys.* **50**, 2383 (2011) [arXiv:1006.2210 [gr-qc]].
 - [25] R. Lazkoz, R. Martens, E. Majerotto, *Phys. Rev. D* **74**, 083510 (2006). [arxiv:astro-ph/0605701].
 - [26] A. Lue and G.D Starkman, *Phys. Rev. D* **70**, 101501 (2004) [arXiv:astro-ph/0408246].
 - [27] P. L. Chimento, R. Lazkoz, R. Maartens, I. Quiros, *JCAP***09**, 004 (2006). [arxiv:astro-ph/0605450].

- [28] M. Bouhmadi-Lopez and R. Lazkoz Phys. Lett. B **654**, 51 (2007). [arXiv:astro-ph/0706.3896].
- [29] H. Zhang and Z. H. Zhu, Phys. Rev. D **75**, 023510 (2007).
- [30] X. Wu, R. G. Cai, and Z. H. Zhu Phys. Rev. D **77**, 043502 (2008).
- [31] J. Wainwright, G. F. R. Ellis, *Dynamical Systems in Cosmology*. (Cambridge University Press, 1997).
- [32] A. A. Coley, *Dynamical systems and cosmology*. (Kluwer Academic Publishers, Dordrecht Boston London, 2003).
- [33] C. G. Boehmer, G. Caldera-Calbral, R. Lazkoz, R. Maartens, Phys. Rev. D **78** 023505 (2008). [arxiv:gr-gc 0801.1565]
- [34] Z. K. Guo, R. G. Cai, Y. Z. Zhang, JCAP**05**, 002 (2005). [arxiv:astro-ph/0412624]
- [35] N. Mahata and S. Chakraborty, Mod. Phys. Lett. A **30**, no. 27, 1550134 (2015).
- [36] S. K. Biswas and S. Chakraborty, Int. J. Mod. Phys. D **24**, no. 07, 1550046 (2015)
- [37] S. K. Biswas and S. Chakraborty, Gen. Rel. Grav. **47**, 22 (2015)
- [38] M. Shahalam, S. D. Pathak, M. M. Verma, M. Y. Khlopov and R. Myrzakulov, Euro. Phys. J. C75 **8**, 395 (2015). [arxiv:gr-gc/1503.08712]
- [39] E. J. Copeland, A. R. Liddle and D. Wands, Phys. Rev. D **57**, 4686-4690 (1998) [gr-qc/9711068]
- [40] A. R. Liddle and R. J. Scherrer, Phys. Rev. D **59**, 023509 (1999)[arXiv:astro-ph/9809272]
- [41] S. Tsujikawa and M. Sami, Phys. Lett. B **603**, 113 (2004) [arXiv:hep-th/0409212].
- [42] I. Quiros, R. Garcia-Salcedo, T. Matos, C. Moreno, Phys. Lett. B**670**, 259-265 (2009) [arxiv:gr-gc 0802.3362]
- [43] Y. Leyva, D. Gonzalez, T. Gonzalez, T. Matos, I. Quiros, Phys. Rev. D **80**, 044026 (2009). [arXiv:gr-gc 0909.0281].
- [44] K. Nozari, F. Rajabi, K. Asadi, Class. Quantum. Grav. **29**, 175002 (2012). [arxiv:gr-gc 1208.1666]
- [45] A. D. Miller *et.al.*, Astrophys. J. Lett. **524**, L1 (1999).
- [46] N. Liang, Z. H. Zhu, Research in Astron. Astrophys 497-506 (2011).
- [47] L. Jie-Chao *et al*, Chin. Phys. Lett Vol No. **2**, 802 (2008).
- [48] S. Wiggins, *Introduction to Applied Nonlinear Dynamical Systems and Chaos*. (Springer, New York Heidelberg Berlin, 1990).
- [49] S. H. Strogatz, *Nonlinear Dynamics and Chaos: With Applications to Physics, Biology Chemistry and Engineering* (Westview Press, Boulder, 2001).
- [50] L. Perko, *Differential Equations and Dynamical Systems*. (SpringerVerlag, 1991).
- [51] B. Aulbach, *Continuous and Discrete Dynamics near Manifolds of Equilibria*. (Lecture Notes in Mathematics No. 1058, Springer, 1984).
- [52] N. Roy, N. Banerjee, Euro. Phys. J. Plus. **129**, 162 (2014).
- [53] J. Dutta, H. Zonunmiiwah, Euro. Phys. J. Plus. **130**, 221 (2015).
- [54] A. P. Billiard, A. A. Coley, Phys. Rev D**61**, 083503, 2000. [arxiv:astro-ph/9908224]
- [55] L. Amendola and S. Tsujikawa, *Dark Energy Theory and Observations*, Cambridge University Press, Cambridge UK, (2010).
- [56] N. Roy, N. Banerjee, Annals Phys. **356**, 452 (2015).
- [57] I. Zlatev, L. M. Wang, P. J. Steinhardt, Phys. Rev. Lett.**82**, 896 (1999)[arxiv:astro-ph/9807002]
- [58] A.P. Billyard, *The Asymptotic Behaviour of Cosmological Models Containing Matter and Scalar Fields* (PhD thesis, Dalhousie University, 1999).
- [59] F. Lucchin and S. Matarrese, Phys. Rev. D **32**, 1316 (1985).
- [60] C. Wetterich, Nucl. Phys. B **302**, 668 (1988)
- [61] D. Wands, E. J. Copeland and A. R. Liddle, Ann. N. Y. Acad. Sci. **688**, 647 (1993).
- [62] N. Piazza, S. Tsujikawa, JCAP **0407**, 004 (2004).
- [63] N. Mahata, S. Chakraborty, Gen. Rel. Grav. **46**,1721 (2014).